



This is a repository copy of *Uncertainty analysis on process responses of conventional spinning using finite element method*.

White Rose Research Online URL for this paper:
<http://eprints.whiterose.ac.uk/103635/>

Version: Accepted Version

Article:

Shi, F., Long, H. orcid.org/0000-0003-1673-1193, Zhan, M. et al. (1 more author) (2014) Uncertainty analysis on process responses of conventional spinning using finite element method. *Structural and Multidisciplinary Optimization*, 49 (5). pp. 839-850. ISSN 1615-147X

<https://doi.org/10.1007/s00158-014-1061-7>

Reuse

Unless indicated otherwise, fulltext items are protected by copyright with all rights reserved. The copyright exception in section 29 of the Copyright, Designs and Patents Act 1988 allows the making of a single copy solely for the purpose of non-commercial research or private study within the limits of fair dealing. The publisher or other rights-holder may allow further reproduction and re-use of this version - refer to the White Rose Research Online record for this item. Where records identify the publisher as the copyright holder, users can verify any specific terms of use on the publisher's website.

Takedown

If you consider content in White Rose Research Online to be in breach of UK law, please notify us by emailing eprints@whiterose.ac.uk including the URL of the record and the reason for the withdrawal request.



eprints@whiterose.ac.uk
<https://eprints.whiterose.ac.uk/>

Uncertainty analysis on process responses of conventional spinning using finite element method

F. Shi^a · H. Long^{b*} · M. Zhan^a · H. Ou^c

^a State Key Laboratory of Solidification Processing, Northwestern Polytechnical University, China

^b Department of Mechanical Engineering, The University of Sheffield, UK

^c Department of Mechanical, Materials and Manufacturing Engineering, The University of Nottingham, UK

*Correspondence. e-mail: h.long@sheffield.ac.uk

Abstract Conventional spinning is a widely used metal forming process to manufacture rotationally axis-symmetric and asymmetric products. Considerable efforts have been made to investigate the forming quality of spun parts using the process in recent years. However, inherent uncertainty properties involved in the spinning process are rarely considered in previous studies. In this paper, an uncertainty analysis and process optimisation procedure have been developed and implemented on conventional spinning with 3D Finite Element Method (FEM). Three process variables are randomized by Gaussian distribution to study the probabilistic characteristics of two process responses. Linear and quadratic approximate representations are constructed by Monte Carlo based Response Surface Method (RSM) with Latin Hypercube Sampling (LHS). The Most Probable Point (MPP) method, which has been widely used to estimate the failure probability in other applications, is further developed in this paper to obtain the probability distribution of the system responses. Following an evaluation of the system responses conducted by the MPP method, a control variable method is used to reduce the variance of spun part wall thickness and total roller force to satisfy the 3σ quality requirement. This uncertainty analysis and process optimization procedure can be easily implemented in other metal spinning processes.

Keywords Conventional spinning · Uncertainty analysis · Probabilistic modeling

Uncertainty analysis on process responses of conventional spinning using Finite Element Method

Shi, F.^a, Long, H.^{b,*}, Zhan, M.^a, Ou, H.^c

^aState Key Laboratory of Solidification Processing, School of Materials Science and Engineering, Northwestern Polytechnical University, Xi'an 710072, PR China

^bDepartment of Mechanical Engineering, The University of Sheffield, Sheffield, S1 3JD, UK

^cDepartment of Mechanical, Materials and Manufacturing Engineering, University of Nottingham, Nottingham, ND7 2RD, UK

Abstract

Conventional spinning is a widely used metal forming process to manufacture rotationally axis-symmetric and asymmetric products. Considerable efforts have been made to investigate the forming quality of the spun part of the process in recent years. However, inherent uncertainty properties involved in the spinning process are rarely considered in previous studies. In this paper, an uncertainty analysis and process optimisation procedure have been developed and implemented on conventional spinning with 3D Finite Element Method (FEM). Three process variables are randomized by Gaussian distribution to study the probabilistic characteristics of two process responses. Linear and quadratic approximate representations are constructed by Monte Carlo based Response Surface Method (RSM) with Latin Hypercube Sampling (LHS). The Most Probable Point (MPP) method, which has been widely used to estimate the failure probability in other applications, is further developed in this paper to obtain the probability distribution of the system responses. Following an evaluation of the system responses conducted by the MPP method, a control variable method is used to reduce the variance of spun part wall thickness and total roller force to satisfy the 3σ quality requirement. This uncertainty analysis and process optimisation procedure can be easily implemented in other metal spinning processes.

Keywords: Conventional spinning, Uncertainty analysis, Probabilistic modeling

1. Introduction

Metal spinning processes, including flowing forming, conventional and shear spinning are widely used in manufacturing complex rotationally axis-symmetric and asymmetric products due

*Corresponding author at: Department of Mechanical Engineering, The University of Sheffield, Sheffield, S1 3JD, UK. Tel: +44(0)1142227759

Email address: h.long@sheffield.ac.uk (Long, H.)

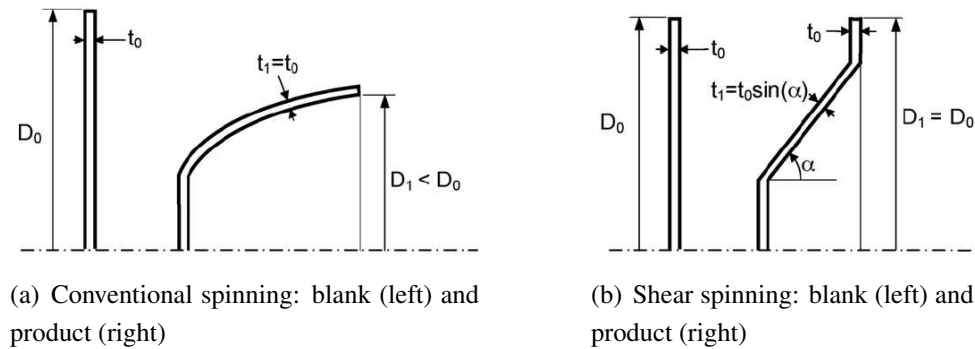


Figure 1: Sheet spinning, adapted from Music et al. (2010)

to its process flexibility, low forming load and high product precision, as summarized by Wong et al. (2003). In the sheet spinning process, the workpiece rotates with the mandrel while one or more rollers revolving around their own axes move along specific roller paths to form the blank onto the mandrel. For the features of conventional spinning shown in Fig.1(a), the workpiece stretches in the radial direction and compresses circumferentially aiming to keep the original wall thickness (t_0) constant during the whole process. For the features of shear spinning shown in Fig.1(b), the final diameter of the blank (D_1) remains constant while the workpiece experiences tensile radial stresses and the final wall thickness (t_1) is reduced according to the sine law, $t_1 = t_0 \times \sin\alpha$, as outlined by Music et al. (2010), where t_0 is the original wall thickness of the blank, α is the inclined angle of the spinning mandrel.

In most cases, the shape and dimensional accuracy of spun parts and the stability of tool forces in the process are two of the most important criteria in spinning process design and production together with other requirements such as spun part surface quality and mechanical strength. It is widely accepted that the wall thickness of blank should theoretically remain constant in conventional spinning, as outlined by Wong et al. (2003). However, many experimental results showed that there was actually a certain amount of thickness variation in conventional spinning process. Quigley and Monaghan (2000) obtained material deformation strains by experimentally measuring the geometry of circles etched on to the blanks before and after spinning. They showed that the measured radial strains were close to the theoretical values while small differences were observed between measured circumferential strains and calculated circumferential strains for a constant thickness. This implies that there exists some thickness strains in the workpiece of conventional spinning, which is also supported by the work of Razavi et al. (2005). Kang et al. (1999) studied the deformation mode of conventional spinning of plates and reported that the deformation of the plates in the first-pass played an important role in the wall thickness distribution of the final part, demonstrating that the thickness of the blank changed

during the process. [Avitzur \(1983\)](#) pointed out that too small a roller nose radius led to poor wall thickness uniformity in conventional spinning. For variations of tool forces during spinning, [Xia et al. \(2005\)](#) showed that axial and radial tool forces increased with the increase of feed rate, by conducting an experimental investigation on a one-pass deep drawing conventional spinning. [Arai \(2003\)](#) used a laser sensor to measure the flange wrinkles and a force transducer to measure the tool forces, indicating that fluctuation of tool forces could be used to detect the initiation of the wrinkling failure. In summary of the studies above, it can be concluded that wall thickness of blank and tool forces do change and vary to some extent in the conventional spinning. In order to achieve high dimensional accuracy of spun components and to control tool force variations in the conventional spinning process, trial and error based iterations are normally used in process design and production. However, this always results in prolonged development time and increased costs due to material wastage as well as the increase of machine and operator's time.

In recent years, FEM has been widely used in the numerical simulation of metal spinning processes. [Hamilton and Long \(2008\)](#) carried out Finite Element simulations of a one-pass deep drawing conventional spinning and the results showed that the circumferential and radial strains did not mirror each other, indicating there were thickness strains existing in the part. The FE analysis of shearing forming process by [Zhan et al. \(2007\)](#) indicated that the larger the feed rate, the less thinning in the wall thickness, which was also supported by [Xia et al. \(2005\)](#). Using numerical simulation and experiment, [Wang and Long \(2011a\)](#) showed that the wall thickness decreased after each forward roller path in a multi-pass conventional spinning process. In their further work, by designing four different roller path profiles including combined concave and convex, convex, linear, and concave, [Wang and Long \(2011b\)](#) conducted FE analyses and spinning experiments to study the effects of the roller path profile on tool force and wall thickness variations in conventional spinning. Furthermore, the thickness distribution of the workpiece in conventional spinning process was analyzed by [Klimmek et al. \(2003\)](#) with FE simulation. The authors found that once the material in the main region of workpiece entered into the local forming zone, the tensile radial stresses could cause the thickness reduction in this area. On the other hand, when the material near the rim of the workpiece came into contact, its significant compressive tangential stresses resulted in material buildup at the front of the roller and led to thickening in the rim of the workpiece.

However, the aforementioned FE simulation works are all based on deterministic methods without consideration of the inherent uncertainties and randomness of process parameter variation in the spinning process. As outlined by [Der Kiureghian and Ke \(1988\)](#), past experience has shown that uncertainties are widely involved not only in the assessment of loading but also in the material and geometric properties of engineering systems. For the conventional spinning process, it involves many random process parameters such as variations of material flow stress,

initial thickness, profile of roller path, roller feed rate and frictional condition between the workpiece and tools. These uncertainties can increase the probability of material failures and geometrical defects of the spun part and scattered distributions of the shape parameters and dimensions of the formed components. In order to achieve high dimensional accuracy of the formed part and ensure the process completes without material failures, it is necessary to analyse and quantify uncertain characteristics of the system response such as variation of spun part wall thickness and tool forces. Stochastic Finite Element method (SFEM) combines the classical deterministic FEM with the stochastic approaches, as reviewed by [Stefanou \(2009\)](#). This method aims at analysing the influence of random system parameters (input) on the uncertainty property of system response (output). In the work published by [Rubinstein and Kroese \(2007\)](#), Monte Carlo Simulation (MCS), the simplest and a universal tool for uncertainty analysis, has been used as a reference approach for validating the results of other methods. However, the application of direct MCS is impossible for large-scale systems and structures due to its excessive computational cost. Therefore, approximation methods deriving from direct MCS such as Monte Carlo based metamodels, Adaptive Monte Carlo simulation have been developed to enable more efficient and robust computational modelling.

Limited investigations have been reported to the use of stochastic approach to quantify the inherent uncertainties in metal forming processes. [Ou et al. \(2011\)](#) developed a two-step FE based stochastic optimization approach for net-shape forging processes. They used a direct compensation method for die shape modification and reduced random variations through a control variable method to keep the die shape and dimensional errors to satisfy the 3σ quality requirement. [Belur and Grandhi \(2004\)](#) studied the uncertainties causing defective parts of hot forging by simulation of deformation process and cooling process, and they illustrated a method which incorporated the process uncertainties into the forging and cooling process design, and controlled the trade-off between rejected parts and rectifiable parts. [Repalle and Grandhi \(2005\)](#) developed a reliability-based optimization method for preform shape design in forging, in which various randomnesses in parameters are quantified and incorporated through reliability analysis and uncertainty quantification techniques. In a research conducted by [Wei et al. \(2008\)](#), a system was considered to be dominated by some of the main effects and lower-order interaction due to the sparsity-of-effect principle. The authors constructed polynomial chaos expansion with points of monomial cubature rules to estimate uncertainty propagation and identified factors contributing to uncertainty. [Jansson et al. \(2008\)](#) used linear and quadratic approximating response surfaces as metamodels to conduct probability analysis for springback and thickness variations in a sheet metal forming process. [Kleiber et al. \(2004\)](#) used a response surface method approach to estimate the probability of sheet metal failures during the forming operation with the influence of uncertainties such as friction, material properties, thickness and blankholding force

studied by the methodology of reliability theory. In a work conducted by [Krusic et al. \(2009\)](#), FE simulations were applied to backward can extrusion, free upsetting, closed-die forging and forward rod extrusion in order to study the effects of scatter of the key process input parameters on the dimensional accuracy of products and on the tool service life. Furthermore, [Rahman and Wei \(2006\)](#) presented a univariate method to approximate multivariate functions by employing the Most Probable Point as the reference point for predicting failure probability of structural and mechanical systems subject to random loads, variations in material properties and geometry. The Most Probable Point (MPP) method was developed to quantify the specific probabilistic distribution of system response by [Du and Chen \(2001\)](#).

Although stochastic approaches combined with FE based methods were applied to carry out uncertainty analysis of some metal forming processes, no research has been reported to consider the inherent uncertainty characteristics of metal spinning processes. In this paper, an uncertainty analysis and process optimisation procedure incorporating FEM was proposed and implemented on the conventional metal spinning process. 3D FE models were validated by experimental results. With probabilistic modeling of three random variables, i.e. material flow stress, roller path and feed rate, linear and quadratic RSM have been applied with LHS methods. The MPP method has been further developed in this paper to study the probability distribution of process response, variations of spun part wall thickness and tool force. The results of these two methods showed good correlations. A system evaluation analysis was carried out to investigate the probability of failures when the process responses were outside the required boundaries. A control variable method was used to optimise the process response to comply with the 3σ quality requirement.

2. Uncertainty Analysis Methods

2.1. Uncertainties of system input and output

System variables (system inputs) include variations of material properties, initial geometrical dimensions and process parameters such as temperature, load and friction conditions. These random system inputs propagate in the whole process and finally lead to the uncertainty characteristics of the system response (output) including variations of dimensional accuracy and microstructures. Therefore the uncertainty analysis aims to find the probability distribution of system response under the effects of the probabilistic properties of system variables (input).

The system response such as the actual geometrical dimensions of a product may be deviated from the desired values. The dimensional error may be given by: $\varepsilon = y - y_0$, where y and y_0 are the actual dimension and the desired value, respectively. A tolerance boundary $[\varepsilon_1, \varepsilon_2]$ of ε is often applied to ensure the actual dimension satisfying the production requirements. Thus $c_2 = \varepsilon_2 + y_0$ and $c_1 = \varepsilon_1 + y_0$ can be the upper boundary (*USL*) and lower boundary (*LSL*) of y , respectively.

The dimension exceeding the USL or LSL is considered as the product failure. It is necessary to control the mean of the system response, μ_y to the desired value y_0 and to minimize the deviation of system response, σ_y . Usually in practical manufacturing, $3\sigma_y$ quality level in Eq.(1) is often used as the eligibility criteria for production processes.

$$LSL \leq \mu_y \pm 3\sigma_y \leq USL \quad (1)$$

2.2. Quantification of the uncertainty characteristics

In the past decades, several methods have been developed in the area of uncertainty analysis. However, conventional spinning process involves a large material plastic deformation, significant dynamic condition and complex interactions between roller and workpiece, which requires an extremely long computational time for 3D FE simulation. Thus computational efficiency and simple implementation are important factors to be considered in this study in selecting uncertainty analysis methods.

2.2.1. Monte Carlo based Response Surface Method

Direct Monte Carlo method is the simplest and most fundamental simulation method in uncertainty analysis (Rubinstein and Kroese, 2007). Inverse transform method is commonly used in MCS to generate random values of system variables according to their probability distributions (Haldar and Mahadevan, 2000), which can be numerically given as:

$$x_{i,j} = F_{X_i}^{-1}(u_{i,j}) \quad i = 1, 2, \dots, p; j = 1, 2, \dots, N \quad (2)$$

where $F_{X_i}^{-1}(x)$ is the inverse cumulative function of system variable x_i , $u_{i,j}$ are selected in region (0, 1) by random number generator; p and N are the number of the system variables and groups of simulations respectively. A larger number of simulations N leads to a higher degree of accuracy of the prediction results. However, it is extremely time-consuming to run a large number of deterministic FE simulations for complex processes such as conventional spinning.

Therefore, a more efficient Monte Carlo based Response Surface Method (RSM) (Myers et al., 2009) was used in this paper together with Latin Hypercube Sampling (LHS) (Helton and Davis, 2003). In this method, deterministic FE simulations are conducted on appropriate Latin hypercube samples of system variables. The response surface can be constructed between the FE simulation results and LH samples by regression analysis. In conventional metal spinning, polynomial regression expansion may be used as the approximate representation and the selected system variables (i.e. material flow stress, roller path profile and feed rate) are considered to be independent from each other, therefore interaction terms could be neglected in the polynomial approximation:

$$y = b_0 + \sum_{i=1}^p b_{1,i}x_i + \sum_{i=1}^p b_{2,i}(x_i)^2 + \dots \quad (3)$$

where y is the system response, constants $b_0, b_{1,i}, b_{2,i} \dots$ can be calculated by the least square method. Then thousands of random samples are generated by inverse transform method similarly to the direct MCS process, while these values are substituted into the Eq.(3) and the results are used to derive the histograms and quantify the uncertainty properties of the system response.

2.2.2. The Most Probable Method

A Most Probable Point (MPP) method was further developed in this paper to estimate the probabilistic distribution of system response. A limit state function can be given as: $g(\mathbf{x}) = y - c$, where c is a constant and $y = h(\mathbf{x})$ is the representation of system response. The system variables \mathbf{x} can be transformed into the standard normal space $\boldsymbol{\alpha}$ by:

$$\alpha_i = \Phi^{-1}[F_i(x_i)] \quad (i = 1, 2, \dots, p) \quad (4)$$

where $F_i(x_i)$ is the cumulative probability function of system variables x_i ; Φ^{-1} is the inverse of a normal distribution function. The limit state function can be rewritten as:

$$g(\boldsymbol{\alpha}) = h(\boldsymbol{\alpha}) - c \quad (5)$$

The most probable point has the shortest distance β from the origin point of the transformed space to the limit state surface $g(\boldsymbol{\alpha}) = 0$, as shown in Fig.2. Eq.(6) can be used to solve the MPP mathematically (Hasofer and Lind, 1974).

$$\beta = \min \|\boldsymbol{\alpha}_{MPP}\| \quad \text{subject to } h(\boldsymbol{\alpha}_{MPP}) - c = 0 \quad (6)$$

where β is referred as the reliable index. The the accurate probability of limit state function less than zero can then be evaluated by:

$$\begin{aligned} P\{g(\boldsymbol{\alpha}) < 0\} &= P\{y = h(\mathbf{x}) < c\} \\ &= \begin{cases} \Phi(\beta) & \text{if } g(\boldsymbol{o}) \leq 0 \\ 1 - \Phi(\beta) & \text{if } g(\boldsymbol{o}) > 0 \end{cases} \end{aligned} \quad (7)$$

where \boldsymbol{o} denotes the origin point in the transformed space. As a result, the probability of failure $P\{y = h(\mathbf{x}) < c\}$ can be evaluated by Eq.(7).

The probabilistic distribution of system response can be further obtained by defining a number of limite state functions (Du and Chen, 2001):

$$p_i = P\{g(\mathbf{x}) < 0\} = P\{y = h(\mathbf{x}) < c_i\} \quad (8)$$

where $i = (1, 2, \dots, n)$. The corrsponding p_i and c_i can be used to construct the cumulative distribution of system response, shown in Fig.3. The solution procedure for points (c_i, p_i) is described as follows:

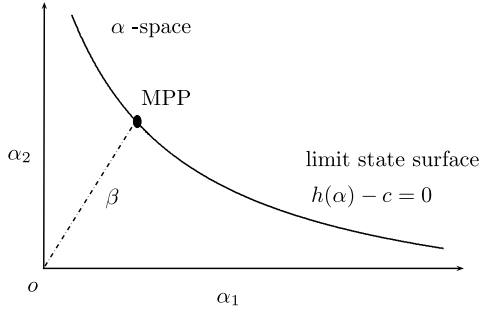


Figure 2: Limit state surface

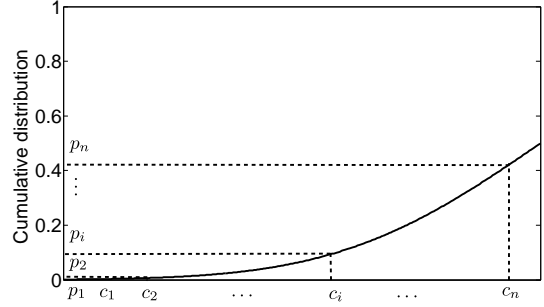


Figure 3: Probability distribution using a set of p and c

- i) A set of p_i ($i = 1, \dots, n$) is selected to reasonably occupy the whole region $[0, 1]$;
- ii) β is a positive value, thus a set of corresponding β_i may be derived by:

$$\begin{aligned} \text{if } p_i \leq 0.5, \quad p_i &= 1 - \Phi(\beta_i) \\ \text{if } p_i > 0.5, \quad p_i &= \Phi(\beta_i) \end{aligned} \quad (9)$$

- iii) As the MPP on the limit state surface has the shortest distance β to the origin point in the α -space, two solutions ($\alpha_i^{(1)}$ and $\alpha_i^{(2)}$) of the vector α_{MPP} can be calculated by:

$$\begin{aligned} \|\alpha_i\| &= \beta_i \\ \alpha_i &\parallel \nabla g(\alpha_i) \end{aligned} \quad (10)$$

where $\nabla g(\alpha)$ is the gradient vector of the limit state surface.

- iv) Corresponding set of constants c_i can be obtained from the limit state surface as following:

$$\begin{aligned} g(\alpha_i^{(1)}) &= h(\alpha_i^{(1)}) - c_i^{(1)} = 0 \\ g(\alpha_i^{(2)}) &= h(\alpha_i^{(2)}) - c_i^{(2)} = 0 \end{aligned} \quad (11)$$

As a result, two values, $c_i^{(1)}$ and $c_i^{(2)}$ are obtained for each p_i . One unreasonable constant in them can be eliminated by:

$$\begin{aligned} \text{if } p_i \geq 0.5 \quad g(\mathbf{o}) &= h(\mathbf{o}) - c_i \leq 0 \\ \text{if } p_i < 0.5 \quad g(\mathbf{o}) &= h(\mathbf{o}) - c_i > 0 \end{aligned} \quad (12)$$

Based on the approximate expression created by RSM, the MPP method can significantly reduce the computational efforts by solving several points (c_i, p_i) , while Monte Carlo based method needs to generate thousands of random samples and to substitute them into the RS equation.

2.3. Control of the uncertainty properties

In this paper, optimisation is conducted on small systematic errors, where μ_y meets $LSL < \mu_y < USL$, however σ_y is too large to satisfy the 3σ quality. A control variable method is used for optimisation to reduce the variance of system response σ_y , demonstrated by Rubinstein and Kroese (2007). For one dimensional case, Y is a response variable correlated with the control variable X . A new response variable, Y_λ , with a smaller variance than that of Y can be constructed as:

$$Y_\lambda = Y - \lambda(X - \mu_X) \quad (13)$$

where μ_X is the known expectation of control variable X , λ is a scalar parameter reducing the variance of control variable X . The variance of new constructed variable Y_λ is given by:

$$Var(Y_\lambda) = Var(Y) - 2\lambda Cov(Y, X) + \lambda^2 Var(X) \quad (14)$$

Consequently, the value λ^* that minimizes $Var(Y_\lambda)$ is

$$\lambda^* = Cov(Y, X)/Var(X) \quad (15)$$

and the minimum variance is

$$Var(Y_\lambda) = (1 - \rho_{YX}^2)Var(Y) \quad (16)$$

where $Cov(Y, X)$ is the covariance of two random variables Y and X , ρ_{YX} is the correlation coefficient of Y and X and the relationship is given as:

$$\rho_{YX} = \frac{Cov(Y, X)}{\sigma_Y \sigma_X} = \frac{E((Y - \mu_Y)(X - \mu_X))}{\sigma_Y \sigma_X} \quad (17)$$

It is clear that the larger $|\rho_{YX}|$ is, the greater influence of the control variable X has on Y , and a higher variance reduction of the response Y can be achieved.

However, in practice, it is actually difficult to meet the target by using single variable control method due to the inherent limit on our ability to control them. Therefore, the method can be extended from single variable control to multiple variables control. Let $\mathbf{X} = (X_1, \dots, X_m)$ be a vector of m control variables, and $\boldsymbol{\lambda}$ is an m -dimensional vector of scalar parameters corresponding to \mathbf{X} . Then Eq.(14) can be rewritten as:

$$Var(Y_\lambda) = Var(Y) - 2\boldsymbol{\lambda}\boldsymbol{\xi}_{YX} + \boldsymbol{\lambda}\boldsymbol{\Sigma}_X\boldsymbol{\lambda}^T \quad (18)$$

Where $\boldsymbol{\xi}_{YX}$ donates the $m \times 1$ vector whose i -th component is the covariance of Y and X_i , and $\boldsymbol{\Sigma}_X$ is the $m \times m$ covariance matrix of \mathbf{X} .

For conventional spinning process, system responses are closely correlated with material properties, geometrical dimensions and key process parameters. By selecting **one or more most influential parameters** and defining the amount of reduction of the variance of each parameter that can be achieved, the overall variance reduction of the system response, i.e. spun part wall thickness and roller force, can be obtained using the proposed control variable method. Thus the probabilistic characteristics of system response would be able to achieve the 3σ quality.

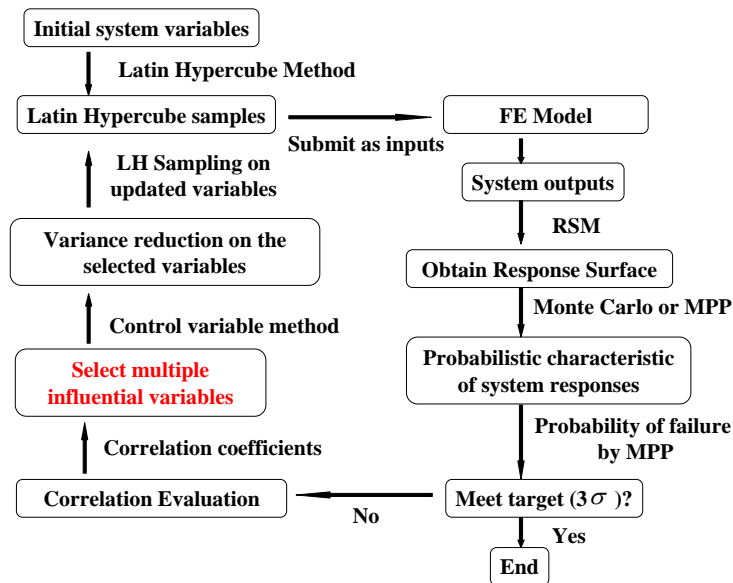


Figure 4: Flow chart of uncertainty analysis and process optimisation procedure

2.4. Developed uncertainty analysis and process optimisation procedure

The flow chart of the developed procedure is shown in Fig.4 and may be described as follows:

- i) Defining the probability distribution of the system variables and selecting a number of random samples by Latin Hypercube method;
- ii) Conducting deterministic FE simulations with all groups of LH samples generated in step i) and then evaluating the system responses;
- iii) Creating RSM between the system variables and responses by regression methods, then quantifying the probabilistic characteristics of system responses by a Monte Carlo method or MPP method;
- iv) Calculating the probability of product failure by MPP method and checking them whether within the 3σ quality. If yes, end the analysis process;
- v) If not, evaluating the correlation coefficients between system variables and responses to **select one or more most influential variables**; then defining the amount of variance reduction of each

variable by the control variable method based on the target variance of the system response. Then goes back to step i) using the updated variables with reduced variance.

3. FE Modeling with Probabilistic Approaches

3.1. Deterministic FE modeling

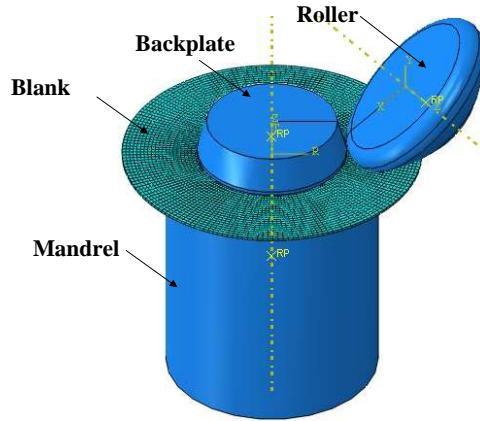
A deterministic FE model of conventional spinning, developed by Wang and Long (2011b), has been further developed to incorporate with the uncertainty analysis in this paper. Due to large material plastic deformation, complex dynamic and frictional contact conditions in the spinning process, the Abaqus/Explicit solution method has been used in the FE simulation. Fig.5(a) shows the FE model in which a single roller with two forward passes and one backward pass is used. Roller, backplate and mandrel are created as analytical rigid bodies. The metal blank is modeled as deformable body meshed by 8-nodes reduced integration linear continuum shell element. Displacement boundary conditions are applied on the roller to complete the three multiple roller passes. The feed rate here refers to the constant feed speed in roller's own axial direction, while the feed speed in roller's own radial direction changes during the whole process according to the specific path profiles. Penalty friction law is used to model the contact behavior between the blank and tools.

Table 1: Conventional spinning parameters

| Parameter | blank diameter (mm) | blank thickness (mm) | spindle speed (rpm) | feed rate (mm/s) | material | Young's modulus (GPa) | Poisson's ratio | Density (kg/m^3) |
|-----------|---------------------|----------------------|---------------------|------------------|----------|-----------------------|-----------------|----------------------|
| Value | 240 | 2 | 400 | 12.65 | DC01 | 198.2 | 0.3 | 7861 |

Table 1 shows key process conditions defined in this FE model. Experimental results obtained from the same process condition are used to validate the results of deterministic FE analysis. Fig.5(b) shows the experimentally spun product. The thickness distributions of experimental and FE results along radial direction are shown in Fig.5(c). Because the actual contact condition between backplate and blank in experiment is more complicated, it may be difficult to precisely simulate the blank deformation near the edge of the backplate. Thus the thickness distribution of the blank between 0 and 0.2 in normalised radial distance can be neglected in the subsequent analysis. As shown in Fig.5(c), it can be seen that the thickness variation trend of FE result shows a good correlation with the variation trend of the experimental result. Both of them increase, then decrease and finally increase towards to the edge of the blank. Furthermore, both sets of the results show that the minimum thickness occurs at the area where the normalised radial distance

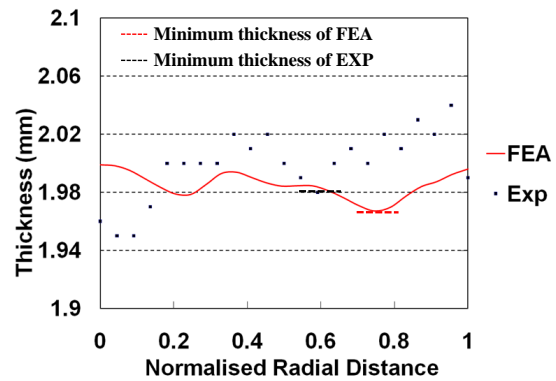
is about 0.6~0.75, as marked by dotted lines. The difference of the minimum thickness between the experimental and FE results is 0.015mm, which may be caused by the inherent uncertainty natures of the real process such as the randomness of the machine precision and uncertainties in the material property.



(a) Conventional spinning FE model



(b) Experimental spun part



(c) Thickness comparison between FE analysis and experimental measurement

Figure 5: Experimental results

3.2. Probabilistic modeling of system variables

Metal spinning process is affected by a number of process parameters including material, geometrical and load factors. In this paper, material flow stress, roller path and feed rate are selected as random variables for uncertainty analysis. All three random variables are assumed to be Gaussian distributed and independent of each other. As a function of plastic strain, material flow stress can be expressed by a random scaling factor k to represent the variation given as: $S = k \times S(\varepsilon)$, where k obeys the normal distribution $N(\mu_k, \sigma_k)$. $S(\varepsilon)$ is the original expression of

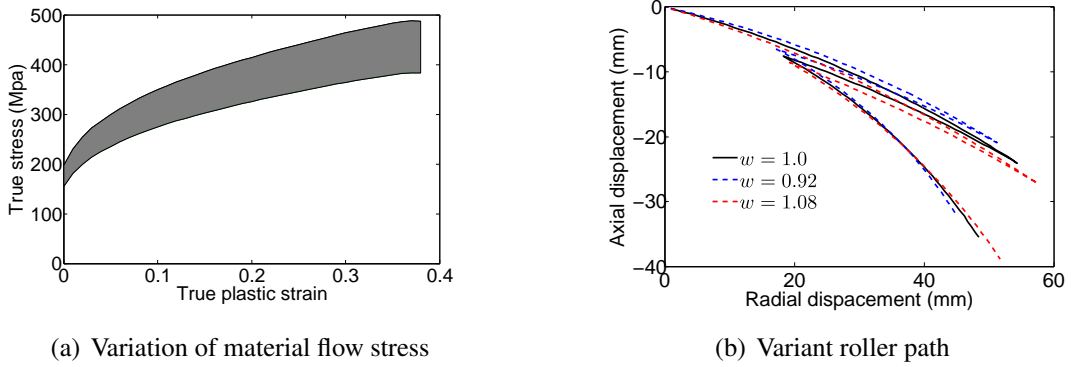


Figure 6: Probabilistic modeling of system variables

material stress and strain relationship. Fig.6(a) shows the defined variation range of flow stress based on this representation. A convex roller path profile containing two forward passes and one backward pass is applied in the FE model. Similarly, the uncertainty of roller path is modeled by defining a random scaling factor, $z = w \times Z(x)$, in which $Z(x)$ is the original roller path profile defined by x and z , where x and z are the radial coordinate and axial coordinate, w is a scaling factor obeying the normal distribution $N(\mu_w, \sigma_w)$. Some examples of variant roller path profiles produced by this method are shown in Fig.6(b). For the feed rate V , it can be directly considered as a normally distributed variable. The specific mean value and standard deviation of each system variable are given in Table 2.

Table 2: Mean value and standard deviation of variables

| | flow stress scaling factor k | roller path scaling factor w | feed rate V (mm/s) |
|-----------------------------|-----------------------------------|-----------------------------------|----------------------|
| mean value μ | 1 | 1 | 12.65 |
| standard deviation σ | 0.04 | 0.03 | 1.33 |

For the Monte-Carlo based RSM, Latin Hypercube Sampling (LHS) method is used to generate 24 sets of random system inputs of the three independent system variables. Then Direct Monte Carlo sampling method is used to generate another large size sample of 3000×3 matrix with three columns representing the three system variables.

4. Results and Discussion

4.1. Probabilistic characterisation of part wall thickness

After running a FE model with the stochastic mean values of the three system variables listed in Table 2, the thickness field distributions at the end of each roller pass are shown in Fig.7. It shows

that the part wall thickness is significantly reduced during 1st forward pass (Fig.7 (a)-(b)) and 2nd forward pass (Fig.7 (c)-(d)), while the thickness remains nearly constant during the backward pass (Fig.7 (b)-(c)). It is probably because the two forward paths have greater curvatures than the backward path, shown in Fig.6(b), causing considerable material deformation. After undergoing three multi-passes conventional spinning, the minimum thickness of the spun part occurs in region A locating towards the outer edge of the workpiece as shown in Fig.7(d).

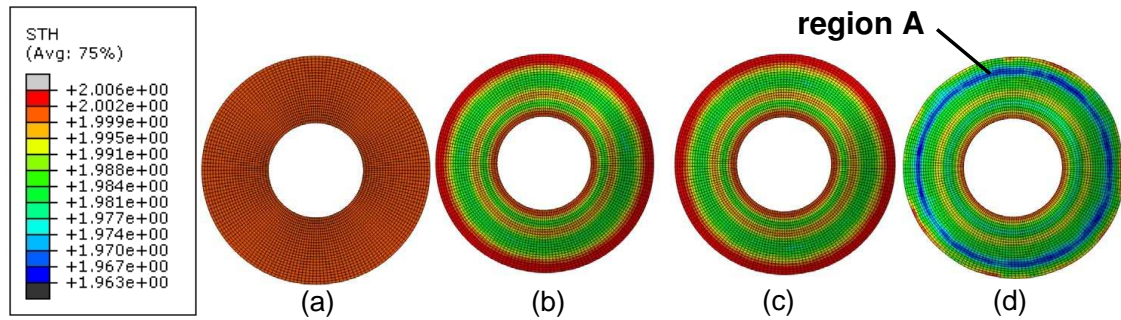


Figure 7: Thickness distribution at different stages: (a) Beginning (b) End of 1st forward pass (c) End of the backward pass (d) End of the 2nd forward pass

Furthermore, 24 sets of deterministic FE simulations are conducted with selected LH Samples, and the minimum thickness of spun part is derived from each set of simulation results. Two simulation results are selected from the 24 simulation results, and the thickness distributions along radial direction are shown in Fig.8, together with the spun part in the simulation with the stochastic mean values of the system variables. It shows that the uncertainties of the system variables have significant effects on the variance of the minimum thickness. Considering this, the minimum thickness of the final spun part is taken as a critical system response, and its probabilistic characteristics are quantified by following uncertainty analysis.

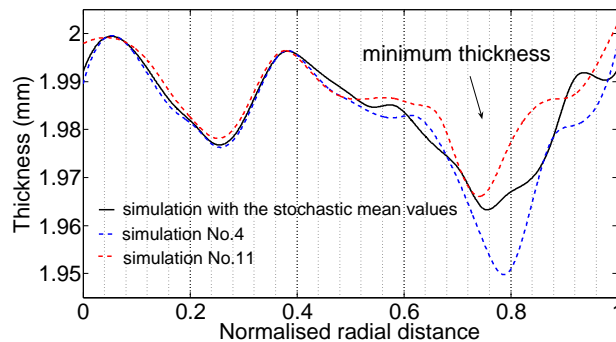


Figure 8: Comparison of thickness distribution along radial direction

4.1.1. Monte Carlo based Response Surface Method

Using the 24 results of minimum thickness obtained from 24 FE models with corresponding LH random inputs, the regression analysis is conducted to obtain the linear and quadratic RSM approximate representation. 3000 Monte Carlo random samples are substituted into each RSM equation and the calculated results are used to derive the histograms and their fitted probability density functions (PDF), shown in Fig.9(a) and Fig.9(b). It shows that the minimum thickness response is also Gaussian distributed by linear approximation in Fig.9(a), while the PDF of quadratic approximation in Fig.9(b) slightly deviates from the normal distribution due to the second order effects. However, minimal differences of mean value and standard deviation are observed between linear and quadratic approximations, which are only 0.01% and less than 8.8% respectively. Thus the two approximate representations by RSM are considered to be valid. To evaluate the correlation between the minimum thickness response and selected system variables, the correlation coefficients are calculated to be: $\rho_{t,k} = 0.1706$, $\rho_{t,w} = -0.3972$ and $\rho_{t,V} = 0.9017$, respectively. It shows that feed rate has the biggest influence on the thickness, while the effect of material flow stress is smallest.

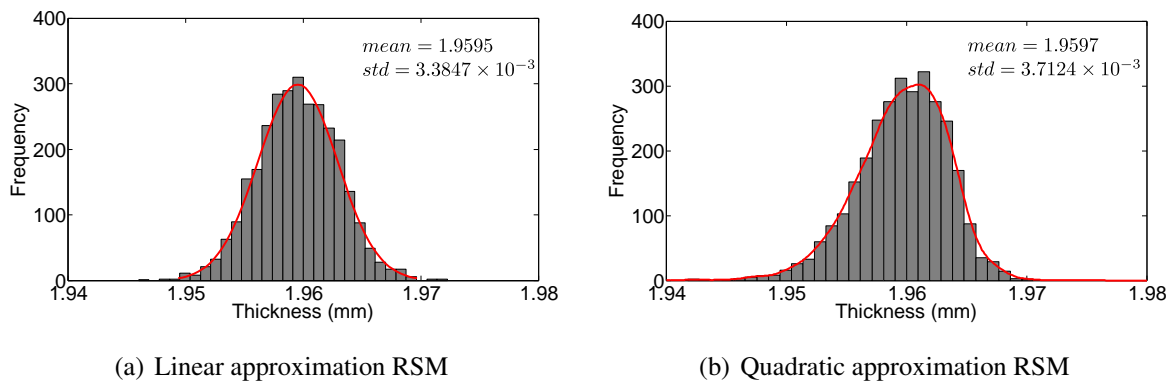


Figure 9: Histogram and fitted PDF of minimum thickness by RSM

4.1.2. Most Probable Point

Based on the linear approximation, the MPP method described in section 2.2.2 is developed to obtain the probability distribution of the minimum thickness and then to conduct system evaluation analysis. Fig.10 compares PDFs of Monte Carlo RSM and MPP method. Based on the same linear approximation, MPP results show a good correlation with corresponding RSM results.

For the system evaluation analysis, a lower tolerance limit of thickness is specified as: $\varepsilon_1 = -0.047$ mm, which means that the lower limit boundary of minimum thickness is: $LSL = t_0 - |\varepsilon_1| = 2 - 0.047 = 1.953$ mm, The limit state function of minimum thickness based on linear RSM can be

given as:

$$g(t_{\min}) = (1.9609 + 1.4288 \times 10^{-2}k - 4.4344 \times 10^{-2}w + 2.2654 \times 10^{-3}V) - 1.953 \quad (19)$$

The reliable index β is calculated to be 1.9443 and this suggests that the probability of failure $P\{g(t_{\min}) < 0\} = 2.59\%$, which is not able to satisfy the 3σ quality.

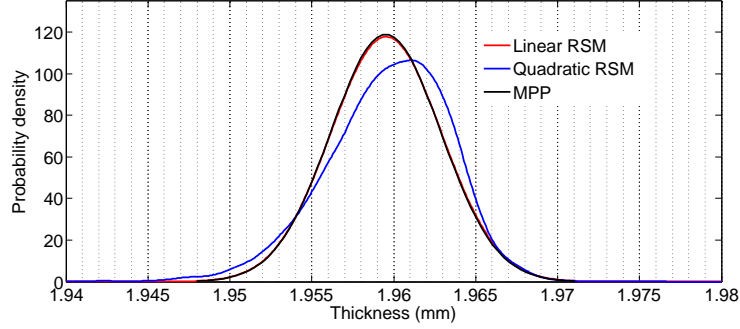


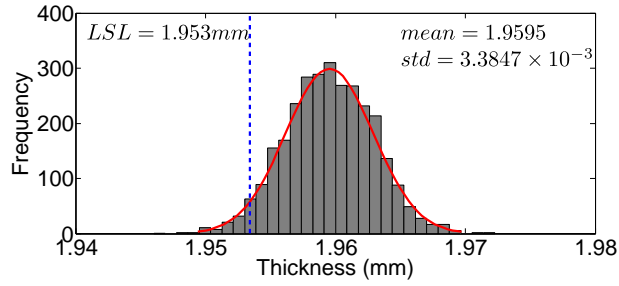
Figure 10: PDF comparison of minimum thickness response between RSM and MPP

4.1.3. Reduction of random variation

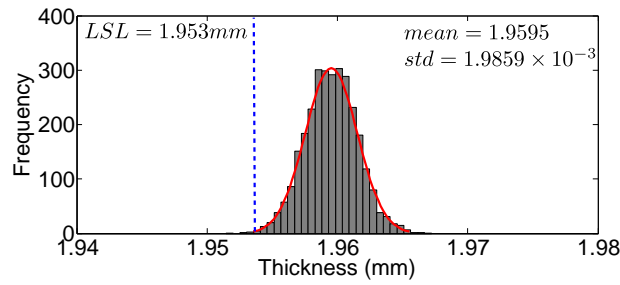
The control variable method described in section 2.3 is applied to reduce the variance of thickness response. Feed rate V is selected as the control variable due to its biggest effect on thickness variation. Based on Eq.(14), the variance of feed rate is calculated to be reduced from $\sigma_V = 1.33$ to $\sigma_V = 0.6$. After another iteration of RSM using the updated feed rate $V \sim N(12.65, 0.6^2)$, a much smaller variance of the thickness response is obtained as shown in Fig.11. The probability of failure is evaluated to be $P\{g(t_{\min}) < 0\} = 0.052\%$ by MPP analysis, which now satisfies the 3σ quality.

4.2. Probabilistic characterisation of total roller force

In spinning process, roller force variations should be controlled in a reasonable range to ensure the stability of the forming process. Similar to the analysis of spun part wall thickness, the results of the same 24 sets of deterministic FE simulations are used and the maximum total roller force of each simulation is obtained. Two simulation results are selected from the 24 sets, and they are compared in Fig.12 together with the simulation result from the stochastic mean values of the random system variables listed in Table 2. It is clear that the uncertainties of the system variables significantly affect the variation of the maximum roller force in the spinning process. The maximum roller force occurs in the 2nd forward pass, which may be caused by the greater curvature of the 2nd forward path shown in Fig.6(b). The probabilistic characteristics of the maximum total roller force in the spinning process are studied with following uncertainty analysis.



(a) Minimum thickness from original linear RSM



(b) Minimum thickness after variance reduction

Figure 11: Comparison of minimum thickness before and after variance reduction

4.2.1. Monte Carlo based Response Surface Methods

Similar to the analysis of spun part wall thickness, the RSM linear and quadratic representations are produced. The 3000 MCS random samples are used to derive the histograms. The fitted PDFs of linear and quadratic RSM are shown in Fig.13. Similar to the thickness response, the maximum roller force response is also normally distributed and no significant differences of the mean value and standard deviation exist between linear and quadratic approximations. The correlation coefficients are calculated to evaluate the correlation between the maximum roller force and system variables: $\rho_{F,k} = 0.8374$, $\rho_{F,w} = -0.4232$ and $\rho_{F,V} = -0.3459$. It suggests that the variance of material flow stress has a much bigger influence on roller forces than the variances of roller path and feed rate, however, the roller path has a slightly greater effect than that of the roller feed rate.

4.2.2. Most Probable Point approach

Similar to the analysis of thickness, Fig.13 presents the comparison of PDFs obtained from RSM and MPP. It shows that MPP method correlates well with the linear approximate RSM.

In the system evaluation analysis, an upper boundary of roller force is specified as: $USL =$

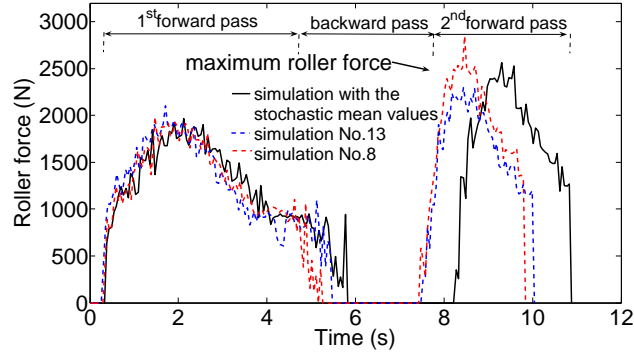


Figure 12: Total roller force in spinning process

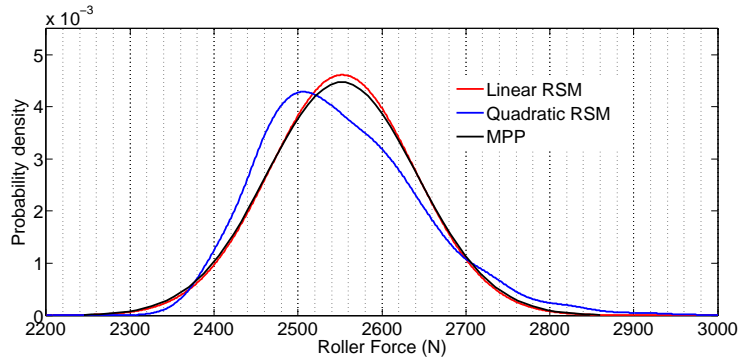


Figure 13: PDF comparison of roller force response between RSM and MPP

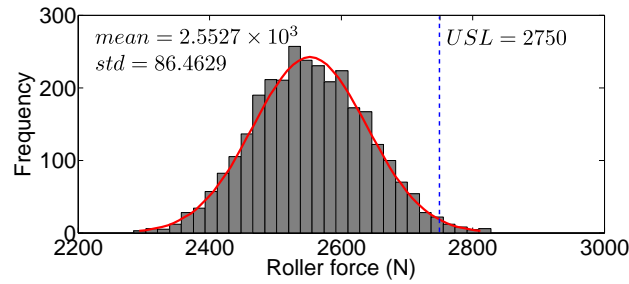
2750N. Thus the limit state function based on linear RSM representation is given as:

$$g(F_{max}) = (2.2361 \times 10^3 + 1.8659 \times 10^3 k - 1.2571 \times 10^3 w - 2.3122 \times 10^1 V) - 2.75 \times 10^3 \quad (20)$$

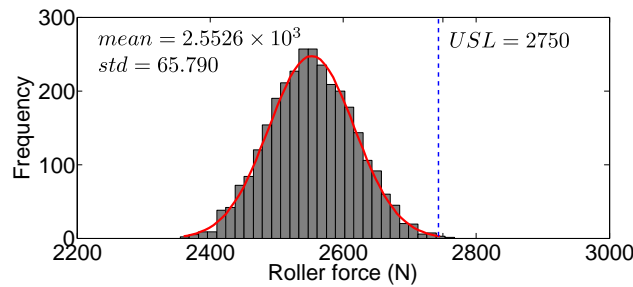
The reliable index is calculated to be 2.2174, which implies that the probability of qualified process is $P\{g(F_{max}) < 0\} = 98.67\%$. However, it still does not satisfy the 3σ quality.

4.2.3. Reduction of random variation

Multiple variable control method is applied to control the scaling factors of material flow stress k and roller path w . Based on Eq.(18) and the target variance of maximum roller force, the variance of k and w can be reduced from $\sigma_k = 0.04$ to $\sigma_k = 0.028$ and $\sigma_w = 0.03$ to $\sigma_w = 0.0203$, respectively. The standard deviation of maximum roller force is reduced considerably after conducting another iteration of the linear approximate RSM with updated variables $k \sim N(1, 0.028^2)$ and $w \sim N(1, 0.0203^2)$, as illustrated in Fig.14. The probability of qualified process is now evaluated to be $P\{g(F_{max}) < 0\} = 99.87\%$ by MPP analysis, which meets the 3σ quality.



(a) Roller force from original linear RSM



(b) Roller force after variance reduction

Figure 14: Comparison of maximum roller force response before and after variance reduction

5. Conclusions

In this research, by applying MCS, RSM, MPP and the control variable methods, an uncertainty analysis method and process optimisation procedure coupled with 3D deterministic FE simulation is developed and implemented on conventional spinning process with multiple roller passes. The following conclusions may be drawn from the results obtained:

- i) The minimum thickness and maximum tool force derived from the linear RSM are normally distributed, while the results of quadratic representation slightly deviate from the normal distribution. The differences between these two approximations are minimal suggesting these two representations are valid. The results of MPP method show a good correlation with linear RSM.
- ii) The uncertainty of process variables significantly affect the variation of the minimum thickness and maximum roller force. Among the three process variables, the uncertainty of feed rate has the biggest effect on the thickness reduction while the material flow stress is the most influential factor for the variance of the total roller force.
- iii) The two forward roller passes produce a higher amount of thickness reduction and higher total roller force than the backward roller pass. The greater curvatures of two forward passes are believed to be the main cause of considerable thinning in wall thickness and higher roller

force.

- iv) Single and multiple variable control methods are proved to be effective to optimise the process responses. The variation of minimum thickness and maximum roller force can be controlled to satisfy the 3σ quality requirement.

6. Acknowledgments

The authors would like to acknowledge the funding supports from the Postgraduate Exchange Programme of Northwestern Polytechnical University, China and EU Marie Curie Actions - MatProFuture Project (FP7-PEOPLE-2012-IRSES-318968).

References

- Arai, H., 2003. Robotic metal spinning-shear spinning using force feedback control, in: Robotics and Automation, 2003. Proceedings. ICRA'03. IEEE International Conference on, IEEE. pp. 3977–3983.
- Avitzur, B., 1983. Handbook of metal-forming processes. John Wiley and Sons, New York, NY .
- Belur, B., Grandhi, R., 2004. Geometric deviations in forging and cooling operations due to process uncertainties. *Journal of materials processing technology* 152, 204–214.
- Der Kiureghian, A., Ke, J., 1988. The stochastic finite element method in structural reliability. *Probabilistic Engineering Mechanics* 3, 83–91.
- Du, X., Chen, W., 2001. A most probable point-based method for efficient uncertainty analysis. *Journal of Design and Manufacturing Automation* 1, 47–65.
- Haldar, A., Mahadevan, S., 2000. Reliability assessment using stochastic finite element analysis. Wiley.
- Hamilton, S., Long, H., 2008. Simulation of effects of material deformation on thickness variation in conventional spinning. In: Proceedings of ICTP2008 (the 9th International Conference of Technology of Plasticity), South Korea , 735–740.
- Hasofer, A., Lind, N., 1974. Exact and invariant second-moment code format. *Journal of the Engineering Mechanics Division* 100, 111–121.
- Helton, J., Davis, F., 2003. Latin hypercube sampling and the propagation of uncertainty in analyses of complex systems. *Reliability Engineering & System Safety* 81, 23–69.
- Jansson, T., Nilsson, L., Moshfegh, R., 2008. Reliability analysis of a sheet metal forming process using monte carlo analysis and metamodels. *Journal of materials processing technology* 202, 255–268.
- Kang, D., Gao, X., Meng, X., Wang, Z., 1999. Study on the deformation mode of conventional spinning of plates. *Journal of Materials Processing Technology* 91, 226–230.
- Kleiber, M., Knabel, J., Rojek, J., 2004. Response surface method for probabilistic assessment of metal forming failures. *International journal for numerical methods in engineering* 60, 51–67.
- Klimmek, C., Gobel, R., Homberg, W., Kantz, H., Matthias, K., 2003. Finite element analysis of sheet metal forming by spinning. *JOURNAL-JAPAN SOCIETY FOR TECHNOLOGY OF PLASTICITY* 44, 372–374.
- Krusic, V., Masera, S., Pristovsek, A., Rodic, T., 2009. Adjustment of stochastic responses of typical cold forging systems. *Journal of Materials Processing Technology* 209, 4983–4993.
- Music, O., Allwood, J., Kawai, K., 2010. A review of the mechanics of metal spinning. *Journal of materials processing technology* 210, 3–23.

- Myers, R.H., Montgomery, D.C., Anderson-Cook, C.M., 2009. Response surface methodology: process and product optimization using designed experiments. volume 705. Wiley.
- Ou, H., Wang, P., Lu, B., Long, H., 2011. Finite element modelling and optimisation of net-shape metal forming processes with uncertainties. *Computers & Structures* 91, 13–27.
- Quigley, E., Monaghan, J., 2000. Metal forming: an analysis of spinning processes. *Journal of Materials Processing Technology* 103, 114–119.
- Rahman, S., Wei, D., 2006. A univariate approximation at most probable point for higher-order reliability analysis. *International journal of solids and structures* 43, 2820–2839.
- Razavi, H., Biglari, F., Torabkhani, A., 2005. Study of strains distribution in spinning process using fe simulation and experimental work, in: *Proceedings of the Tehran International Congress on Manufacturing engineering*, Tehran, Iran.
- Repalle, J., Grandhi, R.V., 2005. Reliability-based preform shape design in forging. *Communications in numerical methods in engineering* 21, 607–617.
- Rubinstein, R., Kroese, D., 2007. *Simulation and the Monte Carlo method*. volume 707. Wiley-interscience.
- Stefanou, G., 2009. The stochastic finite element method: past, present and future. *Computer Methods in Applied Mechanics and Engineering* 198, 1031–1051.
- Wang, L., Long, H., 2011a. Investigation of material deformation in multi-pass conventional metal spinning. *Materials & Design* 32, 2891–2899.
- Wang, L., Long, H., 2011b. A study of effects of roller path profiles on tool forces and part wall thickness variation in conventional metal spinning. *Journal of Materials Processing Technology* 211, 2140–2151.
- Wei, D., Cui, Z., Chen, J., 2008. Uncertainty quantification using polynomial chaos expansion with points of monomial cubature rules. *Computers & Structures* 86, 2102–2108.
- Wong, C., Dean, T., Lin, J., 2003. A review of spinning, shear forming and flow forming processes. *International Journal of Machine Tools and Manufacture* 43, 1419–1435.
- Xia, Q., Shima, S., Kotera, H., Yasuhuku, D., 2005. A study of the one-path deep drawing spinning of cups. *Journal of materials processing technology* 159, 397–400.
- Zhan, M., Yang, H., Zhang, J., Xu, Y., Ma, F., 2007. 3d fem analysis of influence of roller feed rate on forming force and quality of cone spinning. *Journal of materials processing technology* 187, 486–491.